

# Analysis of alternative splicing associated with aging and neurodegeneration in the human brain

James R. Tollervey,<sup>1</sup> Zhen Wang,<sup>1</sup> Tibor Hortobágyi,<sup>2</sup> Joshua T. Witten,<sup>1</sup> Kathi Zarnack,<sup>3</sup> Melis Kayikci,<sup>1</sup> Tyson A. Clark,<sup>4</sup> Anthony C. Schweitzer,<sup>4</sup> Gregor Rot,<sup>5</sup> Tomaž Curk,<sup>5</sup> Blaž Zupan,<sup>5</sup> Boris Rogelj,<sup>2</sup> Christopher E. Shaw,<sup>2</sup> and Jernej Ule<sup>1,6</sup>

<sup>1</sup>MRC Laboratory of Molecular Biology, Hills Road, Cambridge CB2 0QH, United Kingdom; <sup>2</sup>MRC Centre for Neurodegeneration Research, King's College London, Institute of Psychiatry, De Crespigny Park, London SE5 8AF, United Kingdom; <sup>3</sup>EMBL–European Bioinformatics Institute, Wellcome Trust Genome Campus, Hinxton, Cambridge CB10 1SD, United Kingdom; <sup>4</sup>Expression Research, Affymetrix, Inc., Santa Clara, California 95051, USA; <sup>5</sup>Faculty of Computer and Information Science, University of Ljubljana, Tržaška 25, SI-1000 Ljubljana, Slovenia

Age is the most important risk factor for neurodegeneration; however, the effects of aging and neurodegeneration on gene expression in the human brain have most often been studied separately. Here, we analyzed changes in transcript levels and alternative splicing in the temporal cortex of individuals of different ages who were cognitively normal, affected by frontotemporal lobar degeneration (FTLD), or affected by Alzheimer's disease (AD). We identified age-related splicing changes in cognitively normal individuals and found that these were present also in 95% of individuals with FTLD or AD, independent of their age. These changes were consistent with increased polypyrimidine tract binding protein (PTB)–dependent splicing activity. We also identified disease-specific splicing changes that were present in individuals with FTLD or AD, but not in cognitively normal individuals. These changes were consistent with the decreased neuro-oncological ventral antigen (NOVA)–dependent splicing regulation, and the decreased nuclear abundance of NOVA proteins. As expected, a dramatic down-regulation of neuronal genes was associated with disease, whereas a modest down-regulation of glial and neuronal genes was associated with aging. Whereas our data indicated that the age-related splicing changes are regulated independently of transcript-level changes, these two regulatory mechanisms affected expression of genes with similar functions, including metabolism and DNA repair. In conclusion, the alternative splicing changes identified in this study provide a new link between aging and neurodegeneration.

[Supplemental material is available for this article.]

Alzheimer's disease (AD) and frontotemporal lobar degeneration (FTLD) are two of the most common neurodegenerative disorders, each having a distinctive pathology (van der Zee et al. 2008). The prevalence of neurodegenerative diseases increases with age, and molecular processes associated with brain aging contribute to cognitive decline (Bishop et al. 2010). Even though gene expression in the human brain during aging and disease was most often evaluated by separate studies, most of these studies identified down-regulation of genes associated with metabolic and neuron-specific functions (Lee et al. 2000; Lu et al. 2004; Erraji-Benchekroun et al. 2005; Brooks et al. 2007; Liang et al. 2008; Loerch et al. 2008; Miller et al. 2010; Somel et al. 2010). Computational integration of data from these studies suggested a significant overlap between expression changes occurring in aging and AD (Miller et al. 2008). However, expression changes associated with aging and neurodegeneration have not yet been directly compared in a single study.

Here, we directly compared the gene expression changes associated with aging or with disease in the middle temporal gyrus, a region of the brain cortex that is affected in both FTLD and AD, as demonstrated by neuropathological and imaging studies (Whitwell et al. 2008). We obtained RNA samples from cognitively normal (healthy) individuals with ages ranging from 16 to 102 yr, and

compared these to samples from individuals with pathologically confirmed neurodegenerative diseases. These included individuals with sporadic AD, which is characterized by the deposition of extracellular beta-amyloid plaques and intraneuronal tau tangles; with sporadic FTLD-TDP, which is associated with TAR DNA-binding protein (TARDBP, also referred to as TDP-43) deposition, with familial FTLD-TDP due to mutations in the progranulin gene (*GRN*), and with familial FTLD-tau due to mutations in the microtubule-associated protein tau gene (*MAPT*) (Hutton et al. 1998; Poorkaj et al. 1998; Spillantini et al. 1998; Baker et al. 2006; Cruts et al. 2006; Zhang et al. 2007). Past studies indicated aberrant alternative splicing patterns of ion channel and other genes in the brains of AD patients (Glatz et al. 2006; Heinzen et al. 2007; Anthony and Gallo 2010; Twine et al. 2011). Therefore, we evaluated changes in transcription and alternative splicing in a genome-wide manner.

We identified the same gene expression changes in AD and FTLD. Surprisingly, analysis of samples from healthy individuals of different ages showed that the changes taking place in healthy aging represented a subset of the changes present in neurodegenerative diseases. Thus, the disease-related expression changes could be divided into those that also occur in aging (age-related) and those that only occur in disease (disease-specific). In addition to the transcript-level changes, we uncovered dramatic changes in alternative splicing, involving 5369 exons with a >20% inclusion change. These splicing changes indicated a role for increased PTB activity in the age-related changes and decreased NOVA activity in

<sup>6</sup>Corresponding author.

E-mail [jule@mrc-lmb.cam.ac.uk](mailto:jule@mrc-lmb.cam.ac.uk).

Article published online before print. Article, supplemental material, and publication date are at <http://www.genome.org/cgi/doi/10.1101/gr.122226.111>.

the disease-specific changes. Next, we evaluated the cell-type-specific gene expression and detected a major loss of neuronal gene expression in disease, whereas a more modest decrease in expression of glial- and neuron-specific genes occurred in aging. Finally, Gene Ontology analysis showed that gene expression changes in aging primarily affected metabolic processes, whereas the disease-specific changes affected genes with neuron-specific functions, including synaptic transmission and ion channel genes.

## Results

### Analysis of splicing changes in FTLD-TDP, FTLD-tau, and AD

TARDBP is the major component of neuronal and glial inclusions in the most common form of FTLD (FTLD-TDP) (Neumann et al. 2006; Lagier-Tourenne et al. 2010). To assess whether this coincides with changes in TDP-dependent splicing, we initially performed RT-PCR splicing analysis for exons in five different genes that we recently identified as targets of TARDBP in human SH-SY5Y neuroblastoma cells (Tollervey et al. 2011). We identified significant changes in the splicing of exon 11 in the myocyte enhancer factor 2D gene (*MEF2D*) and exon 11 in the microtubule-associated serine/threonine kinase 2 gene (*MAST2*) in FTLD-TDP ( $P$ -value  $< 0.05$ , two-tailed Student's  $t$ -test, unequal variance) (Supplemental Fig. S1A). The remaining exons with no significant change included exon 9 of the checkpoint with Forkhead and ring finger domains gene (*CHFR*), exon 3 of the polymerase (DNA-directed), delta interacting protein 3 gene (*POLDIP3*), and exon 2 of the ral guanine nucleotide dissociation stimulator-like 1 (*RGL1*). We then evaluated splicing of the *MAST2* and *MEF2D* exons in all RNA samples available to us, including samples from 43 healthy controls, six familial FTLD-tau, four familial FTLD-TDP with *GRN* mutations, 16 sporadic FTLD-TDP, 12 individuals with AD, and three individuals with familial ALS with mutations in the fused in sarcoma gene (*FUS*) (Supplemental Table S1; Vance et al. 2009). Surprisingly, even though most FTLD-tau and AD samples lack TARDBP inclusions, they showed the same splicing changes as the FTLD-TDP samples (Supplemental Fig. S2A). For each exon, the splicing change ( $\Delta\Psi$ ) was calculated as the difference in percent exon inclusion in a specific sample compared to the average inclusion in all healthy samples. Based on the average splicing change of both exons, we selected nine healthy samples ( $\Delta\Psi < 5\%$ ) and 16 disease samples ( $\Delta\Psi > 15\%$ ), including three familial FTLD-TDP with *GRN* mutations, four sporadic FTLD-TDP, three familial FTLD-tau, and six AD samples, for a comprehensive transcriptome-wide splicing analysis using high-resolution Affymetrix AltSplice splice-junction microarrays (Supplemental Fig. S2A; Supplemental Table S1).

It is not known if expression changes that were observed by past studies of AD were specific for AD or are also present in other types of neurodegenerative disorder. Therefore, we used hierarchical clustering to assess how the general trends in our microarray data reflect the effects of different neurodegenerative diseases. To minimize the effects of microarray noise, we focused the clustering analysis on the 1000 exons with the most significant changes in FTLD-TDP samples compared to age-matched cognitively normal individuals. The hierarchical clustering clearly distinguished the cognitively normal samples from the disease samples (Fig. 1A). It did not, however, distinguish between different diseases, indicating that the same splicing changes were present in all disease samples. Therefore, we compared exon inclusion from all FTLD-TDP, FTLD-tau, and AD samples with control data to identify 5369 exons with a significant splicing change in all disease samples

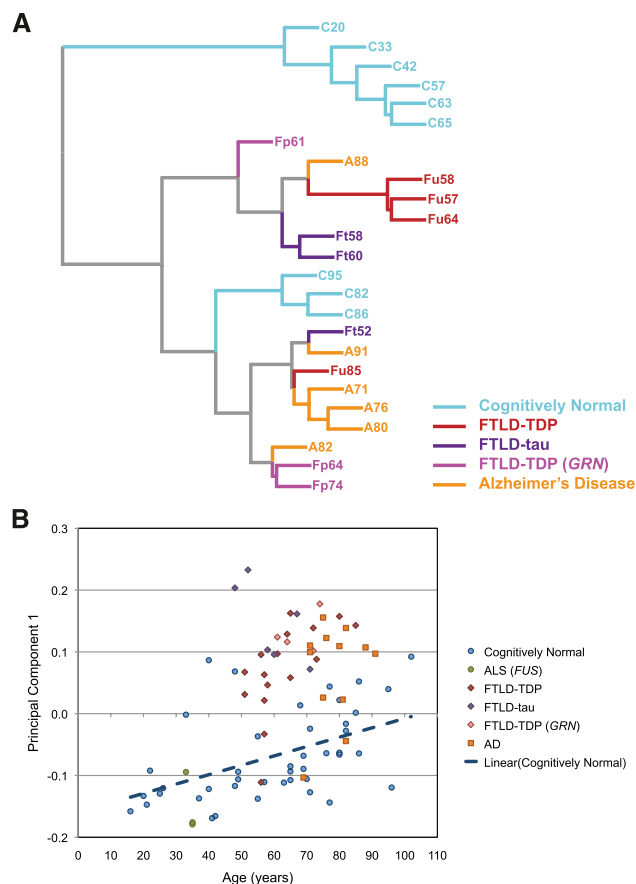


**Figure 1.** Overview of microarray and RT-PCR analyses of splicing profiles. (A) Hierarchical clustering of microarray data [(C) cognitively normal; (Ft) FTLD-tau; (Fp) FTLD-TDP with *GRN* mutation; (Fu) sporadic FTLD-TDP; (AD) Alzheimer's disease], with ages of individuals shown next to disease status. (B) Principal component analysis of RT-PCR data of 13 exons in 84 samples (data shown in Supplemental Fig. S2; Supplemental Tables S1, S2). PC1 values are compared to the age of the donor. The blue line shows the linear regression analysis of the cognitively normal individuals, indicating a trend for a more disease-like splicing pattern with increasing age.

( $P$ -value  $< 0.001$ , one-tailed Student's  $t$ -test, unequal variance,  $\Delta\Psi > 20\%$ ). To evaluate the validity of our microarray measurements, we used RT-PCR to assess splicing changes of 46 randomly selected exons in FTLD-TDP and AD samples. RT-PCR validated 83% (38/46) of these exons, which showed consistent splicing changes in FTLD-TDP and AD ( $P$ -value  $< 0.05$ , one-tailed Student's  $t$ -test, unequal variance) (Supplemental Fig. S1A,B; Supplemental Table S2).

Since only FTLD-TDP samples contain TARDBP inclusions, we hypothesized that these might show some splicing changes associated with TARDBP loss-of-function that are absent in AD. Accordingly, we analyzed the 100 exons with the most significant splicing changes in FTLD-TDP (two-tailed Student's  $t$ -test, unequal variance). Remarkably, all of these exons showed a splicing change in the same direction in both disease types (Supplemental Fig. S1C). The extent of splicing changes for these exons in FTLD-TDP was highly correlated with splicing changes in AD ( $r = 0.95$ , Pearson product moment correlation coefficient). We further searched the microarray data for splicing changes that were specific to FTLD-TDP, but were not able to validate any of these changes by RT-PCR (data not shown). These results indicated that the presence of

TARDBP neuronal and glial inclusions in FTLT-DTP tissues does not associate with a specific splicing signature in the terminal stage of the disease.

To evaluate splicing changes in the whole set of 84 cognitively normal and disease samples available to us, we next used RT-PCR to evaluate the splicing of 13 exons that had the largest splicing changes in FTLT-DTP and AD (Supplemental Fig. S2). We then applied principal component analysis (PCA) to the obtained exon inclusion values to assess the general trends in splicing changes observed in these samples. We found that increasing values of principal component 1 (PC1) distinguished disease samples from healthy control samples, but not between the different disease types (Fig. 1B). This trend was observable with random sampling of as few as five exons out of the 13 exons, indicating that the effect is not specific for only a small subset of the 13 exons (Supplemental Fig. S3A,B). Thus, splicing analysis of a small number of selected exons was sufficient to identify the splicing signature of neurodegeneration.

Interestingly, samples from sporadic and familial FTLT-DTP, FTLT-tau, and AD all had a similar extent of splicing changes, even though the FTLT individuals were generally younger (age range 48–74 yr; mean 63 yr) than the sporadic AD individuals (age range 69–91 yr; mean 78 yr). This observation agrees with magnetic resonance imaging studies reporting accelerated progression of brain atrophy in FTLT when compared to AD (Whitwell et al. 2008). The specificity of our approach was further supported by the observation that splicing in the middle temporal gyrus of ALS (*FUS*) patients, which show motor neuron degeneration in the spinal cord and pre-central gyrus, but no gross pathology in the middle temporal gyrus (Vance et al. 2009), was similar to healthy controls (Fig. 1B). This result confirms that the disease-related splicing changes are a direct effect of neurodegenerative processes in the temporal cortex and not a generalized effect of degeneration elsewhere in the brain.

### Identification of age-related splicing changes

Hierarchical clustering of microarray data indicated that splicing changes in the oldest cognitively normal samples were similar to those in some of the disease samples (Fig. 1A). Furthermore, PCA analysis of RT-PCR values in all 84 samples showed that PC1 values increased with age in healthy controls, resulting in the clustering of older healthy controls closer to the disease samples (Fig. 1B). This suggested that the splicing changes in a subset of healthy samples were age-related. To identify age-related splicing changes on a global scale, we compared the microarray data of the healthy individuals between the ages of 20 and 65 yr with those between the ages of 82 and 95

yr. This identified 1174 exons with a significant splicing change in aging ( $P$ -value  $< 0.001$ , one-tailed Student's  $t$ -test, unequal variance,  $\Delta\Psi > 20\%$ ). Interestingly, age-related splicing changes in these exons were highly correlated with changes in disease ( $r = 0.94$ ). Microarray data identified very few exons with age-related splicing changes that appeared to be absent in disease, but RT-PCR showed that these changes were either not reproducible or were also present in disease samples (Supplemental Table S2). These results indicated that age-related changes represent a subset of the disease-related splicing changes.

Even though all of the changes taking place in aging were also present in disease, the extent of splicing changes varied considerably between aging and disease. Therefore, we speculated that analysis of a disease/aging ratio [DAR = (disease  $\Delta\Psi$ )/(aging  $\Delta\Psi$ )] for each exon could allow a more efficient separation of changes that are primarily associated with aging or neurodegeneration. According to the distribution of these DAR values for all 5369 exons (Supplemental Fig. S3C), we defined thresholds to discriminate the two types of splicing changes. Age-related splicing changes were those present to an almost equal extent in aging and disease (DAR  $< 1.2$ ) (Fig. 2A), whereas changes that were at least twofold greater in disease were considered as disease-specific (DAR

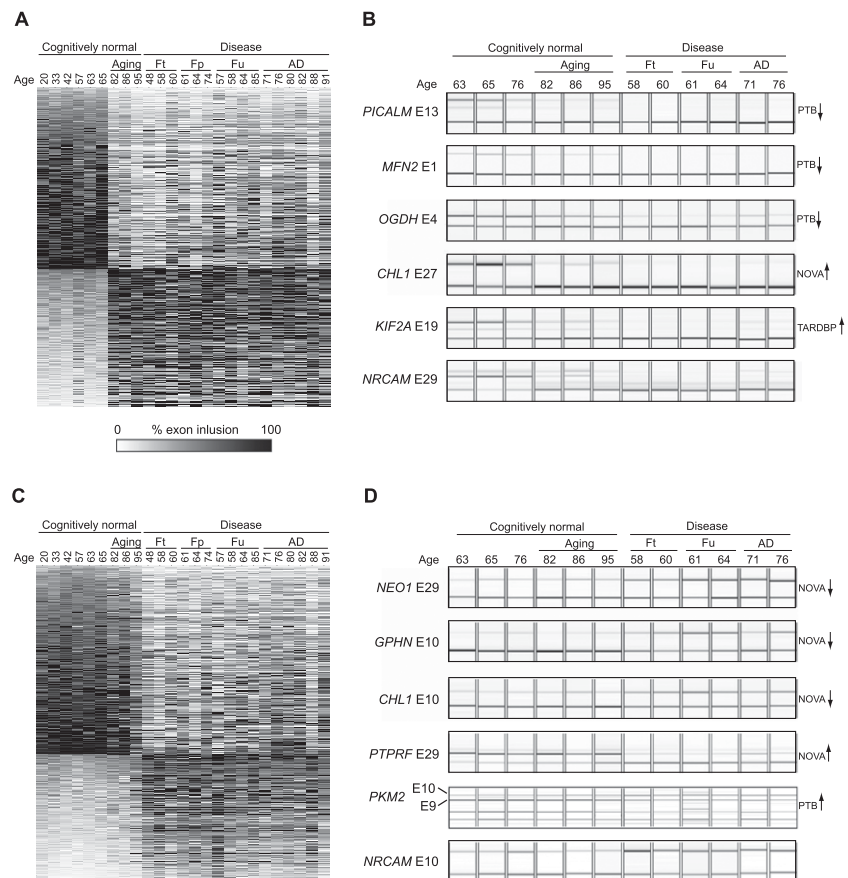


**Figure 2.** Analysis of age-related and disease-specific splicing changes. (A) Heatmap of percentage exon inclusion of the 2064 exons with age-related splicing changes (DAR  $< 1.2$ ). (B) RT-PCR validation of a cohort of the age-associated splicing changes. (C) Heatmap of percentage exon inclusion of the 1551 exons with disease-specific splicing changes (DAR  $> 2$ ). (D) RT-PCR validation of the disease-specific splicing changes. Exons regulated by TARDBP, NOVA, or PTB proteins are labeled on the side, with the enhancing or silencing activity of the protein indicated by an arrow. Age of individual donors and the disease type is shown on top; (Ft) FTLT-tau; (Fp) FTLT-DTP with *GRN* mutation; (Fu) sporadic FTLT-DTP.

> 2) (Fig. 2C). Age-related and disease-specific changes in 12 exons were subsequently confirmed by RT-PCR analyses (Fig. 2B,D), including one TARDBP, five NOVA, and four PTB-target exons (see below).

Interestingly, we observed the occurrence of age-related and disease-specific changes within the same transcript, indicating that different regulatory mechanisms might function at the level of individual exons. To assess this more comprehensively, we identified 107 transcripts that contained more than one exon with age-related or disease-specific splicing changes. Thirty-seven percent of these transcripts (40/107) harbored exons with disease-specific splicing changes, as well as exons with age-related splicing changes. We validated such cases in the cell adhesion molecule with homology with the *L1CAM* gene (*CHL1*) and the neuronal cell adhesion molecule gene (*NRCAM*): Age-related splicing changes were found in *CHL1* exon 27 and *NRCAM* exon 29 (Fig. 2B), and disease-specific splicing changes were found in *CHL1* exon 10 and *NRCAM* exon 10 (Fig. 2D). Since splicing changes in multiple exons in the same transcript can occur at different stages of aging and disease, it is most likely that distinct factors independently regulate each exon.

#### Age-related increase in the PTB-dependent splicing activity

Our results suggest that age-related and disease-specific splicing changes arise from independent regulatory mechanisms acting at the level of individual exons. To explore the roles of candidate splicing regulators, we evaluated exons regulated by TARDBP and TIA proteins. Loss of the nuclear RNA processing function of

TARDBP due to cytoplasmic sequestration has been postulated to underlie neurodegeneration in FTLT-DTP (Neumann et al. 2006; Lagier-Tourenne et al. 2010). Furthermore, TIA proteins (T-cell intracellular antigen 1 [TIA1] and TIA1-like 1 [TIAL1]) are known to respond to cellular stress (Anderson and Kedersha 2002). We have recently identified target exons of TARDBP and TIA proteins using AltSplice microarray analyses upon knockdown in neuroblastoma and HeLa cells, respectively (Wang et al. 2010; Tollervey et al. 2011). We detected disease-related splicing change of 39 exons regulated by TARDBP, 25 of which agreed with decreased TARDBP activity (Supplemental Table S3). We tested splicing of six TARDBP-target exons by RT-PCR, which validated the change measured by the microarray, with four exons having the same direction of splicing change as in the TARDBP knockdown, and two exons having the opposite direction (Fig. 2B; Supplemental Table S2). However, TARDBP- or TIA-target exons were not enriched among disease-related exons (Supplemental Table S3), arguing against a prominent role of these proteins in the observed splicing changes.

To explore the role of additional candidate splicing regulators, we analyzed the transcript levels of genes with ontologies related to splicing regulation as defined by the GO Consortium. This identified 29 genes with a statistically significant, at least twofold disease-related expression change ( $P$ -value < 0.001, one-tailed Student's  $t$ -test, unequal variance) (Table 1). These included several factors involved in PTB-dependent splicing regulation. The expression of polypyrimidine tract binding protein 2 (*PTBP2*) and ribonucleoprotein, PTB-binding 1 (*RAVER1*) was decreased, and expression of regulator of differentiation 1 (*ROD1*) was increased (Rideau et al. 2006; Spellman et al. 2007). The expression of poly-

**Table 1. Splicing regulators with significant disease-related changes in transcript levels**

| Gene symbol    | Gene description  | Disease fold change (log <sub>2</sub> ) | Aging fold change (log <sub>2</sub> ) | Disease/aging fold change ratio |
|----------------|---|---|---------------------------------------|---------------------------------|
| <i>PTBP1</i>   | Polypyrimidine tract-binding protein 1                                      | 0.6                                     | 0.7                                   | 1.0                             |
| <i>ESRP2</i>   | RNA-binding protein 35B   | 1.1                                     | 0.9                                   | 0.9                             |
| <i>ESRP1</i>   | RNA-binding protein 35A   | 1.5                                     | 0.9                                   | 0.7                             |
| <i>RAVER1</i>  | Ribonucleoprotein PTB-binding 1   | 1.2                                     | 0.6                                   | 0.7                             |
| <i>UHMK1</i>   | Serine/threonine-protein kinase Kist  | -1.3                                    | -1.3                                  | 1.0                             |
| <i>DHX15</i>   | Putative pre-mRNA-splicing factor ATP-dependent RNA helicase DHX15          | -1.1                                    | -1.1                                  | 1.0                             |
| <i>HNRNPK</i>  | Heterogeneous nuclear ribonucleoprotein K                                   | -1.1                                    | -0.9                                  | 0.9                             |
| <i>SLU7</i>    | Pre-mRNA-splicing factor SLU7   | -1.2                                    | -1.0                                  | 0.9                             |
| <i>ROD1</i>    | Regulator of differentiation 1  | -1.1                                    | -0.9                                  | 0.9                             |
| <i>PTBP2</i>   | Polypyrimidine tract-binding protein 2                                      | -1.1                                    | -0.8                                  | 0.8                             |
| <i>PLRG1</i>   | Pleiotropic regulator 1   | -1.2                                    | -1.0                                  | 0.8                             |
| <i>SNRPD3</i>  | Small nuclear ribonucleoprotein Sm D3                                       | -1.1                                    | -0.8                                  | 0.8                             |
| <i>SNRNP40</i> | WD-repeat-containing protein 57   | -1.0                                    | -0.8                                  | 0.8                             |
| <i>CUGBP1</i>  | CUG-BP- and ETR-3-like factor 1   | -1.1                                    | -0.8                                  | 0.8                             |
| <i>SFRS2</i>   | Splicing factor, arginine/serine-rich 2                                     | -1.0                                    | -0.7                                  | 0.8                             |
| <i>SRPK1</i>   | Serine/threonine-protein kinase SRPK1                                       | -1.2                                    | -0.8                                  | 0.8                             |
| <i>SRPK2</i>   | Serine/threonine-protein kinase SRPK2                                       | -1.3                                    | -0.9                                  | 0.8                             |
| <i>TXNL4A</i>  | Thioredoxin-like protein 4A   | -1.0                                    | -0.6                                  | 0.7                             |
| <i>WBP11</i>   | WW-domain-binding protein 11  | -1.1                                    | -0.6                                  | 0.7                             |
| <i>SNRNPB2</i> | U2 small nuclear ribonucleoprotein B"                                       | -1.3                                    | -0.8                                  | 0.7                             |
| <i>MAGOH</i>   | Protein mago nashi homolog  | -1.1                                    | -0.5                                  | 0.7                             |
| <i>NUDT21</i>  | Cleavage and polyadenylation specificity factor subunit 5                   | -1.6                                    | -1.1                                  | 0.7                             |
| <i>PIIH</i>    | Peptidyl-prolyl <i>cis</i> -trans isomerase H                               | -1.2                                    | -0.6                                  | 0.6                             |
| <i>NOVA1</i>   | RNA-binding protein Nova-1  | -1.2                                    | -0.5                                  | 0.6                             |
| <i>KHDRBS3</i> | KH-domain-containing, RNA-binding, signal transduction-associated protein 3 | -1.2                                    | -0.6                                  | 0.6                             |
| <i>NHP2L1</i>  | NHP2-like protein 1   | -1.2                                    | -0.4                                  | 0.6                             |
| <i>RNPS1</i>   | RNA-binding protein with serine-rich domain 1                               | -1.3                                    | -0.5                                  | 0.5                             |
| <i>RBM9</i>    | RNA-binding protein 9   | -2.1                                    | -1.3                                  | 0.5                             |
| <i>CDC40</i>   | Pre-mRNA-processing factor 17   | -1.6                                    | -0.7                                  | 0.5                             |
| <i>SNRPN</i>   | Small nuclear ribonucleoprotein-associated protein N                        | -1.9                                    | -0.7                                  | 0.4                             |
| <i>A2BP1</i>   | Fox-1 homolog A   | -2.5                                    | -1.3                                  | 0.4                             |

The fold changes in transcript levels were determined by microarray.

pyrimidine tract binding protein 1 (*PTBP1*) was also significantly increased, even though the increase was only 1.6-fold. These changes agreed with the previous observations that increased *PTBP1* activity is coupled with decreased expression of the *PTBP2* gene (Boutz et al. 2007b; Makeyev et al. 2007; Spellman et al. 2007).

To evaluate PTB-dependent splicing regulation, we analyzed the exons that were identified in a past AltSplice microarray analysis of RNA from *PTBP1/PTBP2* knockdown HeLa cells (Llorian et al. 2010). ASPIRE3 analysis of the microarray data identified a stringent set of 352 PTB-target exons (see Methods). We observed a significant, 2.5-fold enrichment of these PTB-target exons among disease-related exons ( $P$ -value < 0.0001,  $\chi^2$  test with Yates correction) (Table 2). Importantly, 86% (85/99) of these exons changed the splicing pattern in a manner that agreed with increased PTB-dependent splicing activity (Supplemental Table S3). A large proportion of PTB-target exons showed age-related splicing changes, even though their splicing change in disease was generally higher compared to the change in aging (median DAR of 1.97). RT-PCR analysis of five PTB-target exons confirmed that four of these exons had age-related splicing change (Fig. 2B), which agreed with the age-related increase in *PTBP1* expression (Table 1). In conclusion, the age-related splicing changes were consistent with increased PTB-dependent splicing activity, as predicted by changes in transcript levels.

#### Disease-specific decrease in the NOVA-dependent splicing activity

In mouse brain, NOVA proteins play an important role by maintaining brain-specific splicing regulation of transcripts encoding synaptic proteins (Ule et al. 2005; Ruggiu et al. 2009). The micro-

array used in this study evaluated splicing of 51 human orthologs of exons with validated splicing changes in *Nova1<sup>-/-</sup>/Nova2<sup>-/-</sup>* mouse brains (Jensen et al. 2000; Ule et al. 2003, 2005, 2006; Zhang et al. 2010). Ninety-seven percent of the NOVA-binding sites are conserved in vicinity of the human exon orthologs (Jelen et al. 2007), and NOVA2 can change splicing of human exon orthologs (Supplemental Fig. S4). We identified a significant, 3.2-fold enrichment of these human NOVA-target exons among disease-related exons ( $P$ -value < 0.0001,  $\chi^2$  test with Yates correction) (Supplemental Table S3). The median DAR of these exons was 3.55, indicating that their splicing changes were largely disease-specific. We used RT-PCR to test splicing of 25 NOVA-target exons, including some that were not detected as significant by the microarray, and 24/25 were detected as changed in disease samples (Supplemental Fig. S5; Supplemental Table S2). Eighty-three percent (20/24) of NOVA-target exons had disease-specific splicing changes, whereas the remaining four exons also showed significant splicing changes in aging (Fig. 2B,D; Supplemental Fig. S5; Supplemental Table S2). Importantly, all of the splicing changes detected by microarray or RT-PCR had a pattern that agreed with decreased activity of NOVA proteins in disease tissue (Supplemental Tables S2, S3).

We next wanted to explore whether the change in NOVA-dependent splicing was based on altered abundance of the NOVA proteins. Since a past study showed that two-thirds of NOVA proteins are present in the cytoplasmic fraction of the mouse brain (Racca et al. 2010), we evaluated their protein levels in nuclear and cytoplasmic fractions of human brain tissues. Protein levels of NOVA1 and NOVA2 were significantly decreased in both nuclear and cytoplasmic fractions of disease samples (Fig. 3). In contrast, whereas both proteins were significantly decreased in the cytoplasmic fraction of aging samples, their abundance in the nuclear

**Table 2.** GO terms enriched in genes with age-related or disease-specific expression changes

| GO term   | Age-related               |      |                 |      | Disease-specific          |      |                 |      |
|---|---------------------------|------|-----------------|------|---------------------------|------|-----------------|------|
|   | Transcript-level decrease |      | Splicing change |      | Transcript-level decrease |      | Splicing change |      |
|   | <i>P</i> -value           | Fold | <i>P</i> -value | Fold | <i>P</i> -value           | Fold | <i>P</i> -value | Fold |
| Anion transport                                     | 0.012                     | 3.2  |                 | 1.2  |                           | 0.8  |                 | 0.9  |
| Mitochondrial electron transport NADH to ubiquinone | 0.013                     | 5.3  |                 | 1.2  |                           | 2.2  |                 | 2.4  |
| Ribonucleoside monophosphate biosynthetic process   | 0.023                     | 4.8  |                 | 1.1  |                           | 0    |                 | 0.9  |
| Modification-dependent protein catabolic process    | <0.001                    | 4.1  |                 | 1.3  |                           | 0.8  |                 | 0.7  |
| ER to Golgi vesicle-mediated transport              | 0.024                     | 3.3  | 0.027           | 2.0  |                           | 0    |                 | 1.2  |
| S phase   |                           | 0    | 0.030           | 5.1  |                           | 0    |                 | 0.3  |
| tRNA metabolic process                              |                           | 0.9  | <0.001          | 2.1  |                           | 0    |                 | 1.0  |
| G <sub>1</sub> phase                                |                           | 0    | 0.002           | 2.9  |                           | 0    |                 | 0    |
| Nucleotide-sugar metabolic process                  |                           | 2.0  | 0.008           | 3.2  |                           | 0    |                 | 0.6  |
| Non-recombinational repair                          |                           | 0    | 0.011           | 3.0  |                           | 0    |                 | 1.1  |
| Mismatch repair                                     |                           | 0    | 0.030           | 2.4  |                           | 0    |                 | 0.9  |
| Protein heterooligomerization                       |                           | 1.8  | 0.034           | 2.0  |                           | 1.5  |                 | 1.9  |
| Isoprenoid biosynthetic process                     |                           | 3.5  | 0.047           | 2.4  |                           | 0    |                 | 2.1  |
| Transmission of nerve impulse                       |                           | 1.0  |                 | 1.1  | <0.001                    | 7.4  | <0.001          | 2.0  |
| Neurological system process                         |                           | 0.9  |                 | 0.9  | <0.001                    | 4.5  | <0.001          | 1.5  |
| Monovalent inorganic cation transport               |                           | 0.8  |                 | 1.1  | <0.001                    | 5.4  | 0.029           | 1.5  |
| Synaptic vesicle endocytosis                        |                           | 0    |                 | 1.6  | <0.001                    | 14   | <0.001          | 4.7  |
| Regulation of transport                             |                           | 0.8  |                 | 0.5  | <0.001                    | 3.4  | 0.001           | 1.6  |
| Chemical homeostasis                                |                           | 1.2  |                 | 0.7  | <0.001                    | 3.5  | 0.043           | 1.3  |
| Potassium ion transport                             |                           | 0.4  |                 | 0.8  | <0.001                    | 6.5  | 0.034           | 1.8  |
| Response to metal ion                               |                           | 0.5  |                 | 0.8  | 0.008                     | 3.0  | <0.001          | 2.1  |
| Positive regulation of synaptic transmission        |                           | 2.1  | 0.007           | 3.3  | <0.001                    | 13   |                 | 2.5  |
| Sensory perception of pain                          |                           | 1.7  |                 | 1.5  | <0.001                    | 13   |                 | 0.5  |
| Actin polymerization or depolymerization            |                           | 1.3  |                 | 0.5  |                           | 2.2  | <0.001          | 2.5  |
| Isoprenoid metabolic process                        |                           | 2.9  |                 | 1.9  |                           | 0    | 0.034           | 2.3  |
| Peptidyl-threonine phosphorylation                  |                           | 4.0  | 0.029           | 2.7  |                           | 6.6  | 0.002           | 4.1  |

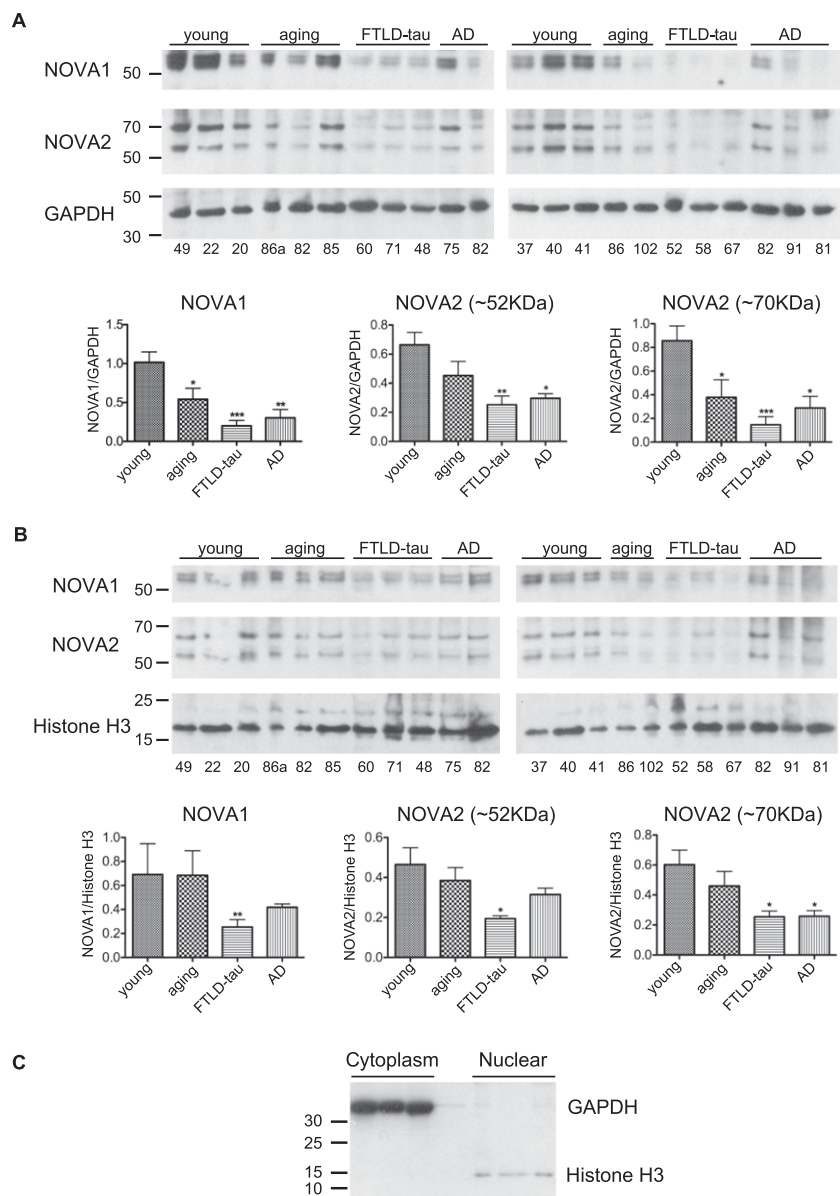


**Figure 3.** Analysis of the nuclear and cytoplasmic abundance of NOVA proteins. A total of six young healthy, five aging healthy, six FTLD-tau, and five AD samples were lysed into cytoplasmic (A) and nuclear (B) fractions. Immunoblot analysis of NOVA1, NOVA2 (detected in two different isoforms of ~52 kDa and 70 kDa), and cytoplasmic (GAPDH) and nuclear (Histone H3) loading controls is shown. Mean and standard deviation of NOVA signal, normalized against the loading controls, is shown in the graphs. Significant difference in NOVA protein abundance is marked; (\*)  $P$ -value < 0.05; (\*\*)  $P$ -value < 0.01; two-sided Student's  $t$ -test, unequal variance. (C) Separation of cytoplasmic and nuclear fractions from human post-mortem samples was efficient. GAPDH was only present in the cytoplasmic fraction, whereas histone H3 was present only in the nuclear fraction.

fraction of aging samples remained unchanged. This unchanged nuclear abundance of NOVA proteins agreed with the intact splicing of most NOVA-target exons in the aging samples.

#### Analysis of cell-type-specific changes in gene expression

Due to neuronal loss in the affected brain tissue, neuron-specific genes have decreased expression in neurodegenerative diseases, but less is known about the role of neuronal loss in the age-related

expression changes. To address this question, we made use of available cell-type-specific gene expression data measured from purified mouse neurons, astrocytes, and oligodendrocytes (Cahoy et al. 2008). Upon assigning corresponding mouse-human orthologs, we assigned genes with a greater than twofold increase in expression as specific for the corresponding cell type. These were compared to the 3061 genes with a significant, at least twofold transcript-level change in disease ( $P$ -value < 0.001, one-tailed Student's  $t$ -test, unequal variance). The latter were further divided into four groups depending on whether they had decreased or increased expression and whether the changes were age-related (disease/aging fold change < 1.2) or disease-specific (disease/aging fold change > 2). In agreement with neuronal loss in neurodegeneration, we saw a 9.6-fold enrichment of neuron-specific genes among genes with a disease-specific decrease in expression (Fig. 4). In contrast, an only 1.9-fold enrichment of neuron-specific genes was observed among genes with age-related decrease in expression, which was similar to the enrichment of glial genes. In fact, oligodendrocyte-specific genes had the greatest enrichment (2.2-fold) among the genes with age-related decrease in expression (Fig. 4). This result indicates that rather than being an indirect result of neuronal loss, the age-related changes result from more specific regulatory mechanisms that affect all brain cell types.

#### Analysis of molecular processes affected by splicing or transcript-level changes

To identify the biological processes affected by the transcript-level and splicing changes, we identified the Gene Ontology terms with significant enrichment ( $P$ -value < 0.05) in genes with age-related or disease-specific changes. Few Gene Ontologies were enriched in genes with transcript-level increases, and these were distinct from those enriched in transcript-level decreases or splicing changes (data not shown). Interestingly, even though Gene Ontologies enriched in genes with age-related splicing changes or transcript-level decreases were mainly related to metabolic processes, the ontologies enriched in splicing and transcript-level changes were different (Table 2; Supplemental Table S4). In addition, age-related splicing changes were enriched in genes with functions in DNA repair. These include non-homologous end-joining factor 1 (*NHEJ1*), mediator of DNA-damage checkpoint 1 (*MDC1*), RAD50 homolog (*RAD50*), RAD51 homolog C (*RAD51C*), DNA helicase Q1-like (*RECQL*), X-ray

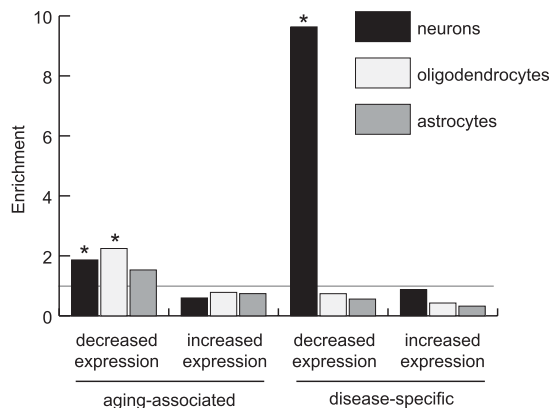


**Figure 4.** Analysis of cell-type-specific gene expression. The y-axis shows the enrichment of cell-type-specific genes (Cahoy et al. 2008) (see Methods) among the genes with increased or decreased age-related or disease-specific changes in transcript levels. (\*) Significant difference in proportion of cell-type-specific genes ( $P$ -value < 0.0001,  $\chi^2$  test with Yates correction).

repair complementing defective repair in Chinese hamster cells 4 and 5 (*XRCC4* and *XRCC5*), mutL homolog 1 (*MLH1*), mutY homolog (*MUTYH*), and APEX nuclease 1 (*APEX1*). In contrast, Gene Ontologies enriched in genes with disease-specific splicing changes or transcript-level decreases were mainly the same, including synaptic transmission and other neuron-related processes (Table 2; Supplemental Table S4). These results indicate that disease-specific transcript and splicing changes are a result of neuronal loss associated with the neurodegeneration, whereas the age-related changes are a result of more specific regulatory mechanisms that target distinct cellular processes.

## Discussion

In the present study, we found that the gene expression changes that take place during aging in the temporal lobe of cognitively normal individuals also occur in individuals with dementia regardless of their age. This allowed us to separate the disease-related changes into two subsets: those that were present in disease, but were much smaller or absent in aging (disease-specific changes); and those that occurred in both disease and aging (age-related changes). Whereas the disease-specific changes indicated severely decreased expression of neuron-specific genes, the age-related changes indicated a slightly decreased expression of genes specific for neuronal and glial cell types. Interestingly, the oligodendrocyte-specific genes had the strongest age-related decrease in expression, which might be related to the oligodendroglial pathology evident in AD (Miller et al. 2010; Mitew et al. 2010). Whereas oligodendrocytes are not thought to be a major cell type in brain cortex, these changes could also involve polydendrocytes (NG2 cells) (Nishiyama et al. 2009).

Analysis of data from multiple studies has shown that expression changes in genes with functions in metabolism and synaptic plasticity are particularly conserved between AD and aging (Miller et al. 2008). Our results were consistent with this observation, but we additionally identified differences in the extent of these changes that discriminate aging from disease. For instance, even though expression of genes with neuron-specific functions was changed in aging, these changes were modest compared to disease. In contrast, genes with metabolic functions changed to the same extent in both

aging and disease. Interestingly, we found that the metabolic ontologies enriched in genes with splicing changes were different from those enriched in genes with transcript-level changes.

A more detailed look at the age-related splicing changes revealed 12 exons in transcripts encoding tRNA synthetases and 19 exons in other transcripts involved in tRNA metabolism. Aberrant splicing of these transcripts might lead to accumulation of mutant proteins with a tendency for misfolding, as has been shown in the case of an RNA editing defect in the alanyl-tRNA synthetase transcript (Lee et al. 2006). In addition, our results indicate that alternative splicing complements the transcriptional regulation in modifying the molecular machinery for the repair of oxidative DNA damage in the brain (Lu et al. 2004; Su et al. 2008). Importantly, age-related splicing changes were identified in several genes in which pathological mutations or functional variants are associated with aging or neurodegenerative disorders. Use of a cryptic splice site in exon 11 of the lamin A (*LMNA*) transcript plays a role in aging, and mutations that increase use of the cryptic splice site cause the premature aging syndrome Hutchinson-Gilford progeria (HGPS) that primarily affects tissues of mesenchymal origin (Scaffidi and Misteli 2006). Microarray data in this study indicated an age- and disease-related change in the use of the *LMNA* alternative promoter. Kinesin family member 1B (*KIF1B*) is the motor protein involved in anterograde transport of mitochondria, and mutations in the respective gene cause Charcot-Marie-Tooth type 2A1 sensory motor neuropathy (Nangaku et al. 1994; Zhao et al. 2001). Mitofusin 2 (*MFN2*) tethers endoplasmic reticulum to mitochondria, and mutations in the respective gene cause CMT type 2A2 (Zuchner et al. 2004; de Brito and Scorrano 2008; Merkwirth and Langer 2008). *FUS* is an RNA- and DNA-binding protein, and mutations in the *FUS* gene cause familial amyotrophic lateral sclerosis (ALS) (Kwiatkowski et al. 2009; Vance et al. 2009). Plastin 3 (*PLS3*) is a protective modifier of autosomal recessive spinal muscular atrophy (Oprea et al. 2008). Finally, mutations in the phosphatidylinositol-binding clathrin assembly protein gene (*PICALM*) are associated with AD (Harold et al. 2009).

To understand regulatory mechanisms involved in the observed splicing changes, we analyzed disease-related changes in the transcript levels of RNA-binding proteins. These included four RNA-binding proteins involved in PTB-dependent splicing regulation. In addition, the age-related splicing changes were consistent with increased PTB-dependent splicing activity. During nervous system development, *PTBP1* and *PTBP2* mRNA levels are under control of several microRNAs, which thereby control the differentiation of neuronal progenitor cells to mature neurons (Boutz et al. 2007a; Makeyev et al. 2007). This is of particular interest due to a recent finding that expression of microRNAs and their target mRNAs links development and aging in human and macaque brain (Somel et al. 2010).

We also detected decreased levels of NOVA proteins in the nuclear and cytoplasmic fractions of disease tissue. Since *NOVA1* and *NOVA2* genes are primarily expressed in neurons (Buckanovich et al. 1996), this result is consistent with the decreased expression of neuron-specific genes in disease. Interestingly, we find that the levels of cytoplasmic, but not nuclear NOVA proteins decrease in an age-related manner. This observation indicates that import of NOVA proteins into the nucleus during aging might be necessary to maintain normal nuclear NOVA function, despite a decrease in the cytoplasmic NOVA protein abundance. However, a decrease in cytoplasmic NOVA proteins might affect neuronal function and thereby contribute to the aging process. For instance, it has been shown that NOVA proteins colocalize with their target RNAs

in neuronal dendrites of mice (Racca et al. 2010). Analysis of NOVA localization in mouse models of neurodegeneration might provide further insights into these questions.

Even though nuclear depletion of TARDBP and its sequestration within cytoplasmic inclusions is evident in FTLD-TDP tissue samples, we did not identify any specific splicing changes associated with FTLD-TDP that would differ from changes present in AD or in FTLD with *MAPT* mutations. Furthermore, splicing changes of TARDBP-target exons in disease tissues did not correlate with changes that were identified in TARDBP knockdown neuroblastoma cells by our previous study (Tollervey et al. 2011). However, this should not be taken as a rejection of the TARDBP loss-of-function hypothesis. It is possible that decreased function of TARDBP in a specific population of affected cells is sufficient to trigger the neurodegenerative process but may not be detected in the whole-tissue analysis. Analysis of splicing from affected neuronal populations might be necessary to detect a signature of TARDBP loss-of-function. We should also point out that in spite of the lack of consistent evidence for the TARDBP loss-of-function hypothesis, we did identify 25 exons that showed the same direction of change in disease tissues as upon knockdown of TARDBP in neuroblastoma cells. These exons locate to several genes involved in apoptosis: BCL2-like 11 (*BCL2L11*, also referred to as BIM), programmed cell death 6 (*PDCD6*), MAP-kinase activating death domain (*MADD*), kinesin family member 1B (*KIF1B*), and phosphofructokinase (*PFKP*) (Zhang et al. 1998; Almeida et al. 2004; Trioulier et al. 2004; Schlisio et al. 2008; Tollervey et al. 2011).

It is important to be aware of the limitations of the data presented in this study. Age-related expression changes are known to diverge among tissues within the same organism (Zahn et al. 2007). It therefore remains to be seen whether brain regions other than the middle temporal gyrus show the same extent of overlap between aging and disease-related expression changes. Furthermore, the exons regulated by the RNA-binding proteins evaluated in this study were originally identified in human cell lines or mouse brain, and therefore some of these exons might not be regulated by the same proteins in human brain. It is likely that some of the observed splicing changes were caused by mechanisms other than changes in the activity of RNA-binding proteins, such as cotranscriptional regulation of alternative splicing that could result from age-related changes in chromatin and DNA damage (Munoz et al. 2009; Pegoraro et al. 2009). Finally, we found changes in transcript levels of multiple RNA-binding proteins. These include important hnRNP and SR proteins, as well as SRPK kinases that phosphorylate SR proteins (Table 1). These proteins are likely to modulate splicing in a combinatorial manner together with PTB and NOVA-family proteins, and further analyses will be required to understand the full regulatory program that orchestrates the aging- and disease-related splicing changes. In conclusion, our data provide new insights into the gene expression changes that distinguish healthy aging from neurodegeneration and identify the candidate regulators of alternative splicing that are associated with both processes.

## Methods

### Brain tissue

Frozen brain tissues were obtained from the MRC London Neurodegenerative Diseases Brain Bank (Institute of Psychiatry, King's College London, UK). Consents for autopsy, neuropathological assessment, and research including genetic studies were obtained

from all subjects in accordance with local and national guidelines for organ donation approved by The Joint South London and Maudsley and the Institute of Psychiatry Research Ethics Committee (#231/01). The randomly selected right or left halves of donated brains were sliced fresh in the coronal plane and were kept frozen at  $-80^{\circ}\text{C}$ . The slice containing the superior sulcal margin of the middle temporal gyrus (Brodmann area 21) at the level of the mammillary body was allowed to slowly reach  $-20^{\circ}\text{C}$  in a freezer. Subsequently 80–100 mg of the neocortex was harvested in a fume cabinet, weighed on a precision scale, and kept at  $-80^{\circ}\text{C}$  in an Eppendorf tube for RNA isolation. Block taking for histological and immunohistochemical studies and neuropathological assessment of disease and healthy cases was performed in accordance with published guidelines by a consultant neuropathologist. As controls, we isolated samples from donated brains of 43 cognitively normal individuals of 16 to 102 yr with no clinical history of a neurodegenerative condition, in particular dementia, and lacking any signs of disease neuropathology.

### Splice-junction microarray

The high-resolution AltSplice splice-junction microarrays were produced by Affymetrix, the cDNA samples were prepared using the GeneChip WT cDNA Synthesis and Amplification kit (Affymetrix 900673), followed by GeneChip Hybridization, Wash, and Stain Kit (Affymetrix 900720) using Affymetrix GeneChip Fluidics Station 450, and scanned on Affymetrix GeneChip Scanner 3000 7G. The resulting cel files were analyzed with the version 3 of ASPIRE (Analysis of Splicing Isoform REciprocity) (König et al. 2010). To identify the most stringent set of exons with splicing changes in *PTBP1/PTBP2* or *TIA1/TIAL2* knockdown cells, we selected those with  $|\Delta I_{\text{rank}}| > 3$ , as calculated by ASPIRE3.

### RT-PCR

The primer pairs (Supplemental Table S2) were designed for exons that were 9–80 nt in length, so that the resulting PCR products were between 70 and 150 nt in length—the small variation in the size of two PCR products ensured minimal effect of the variable RNA quality between the different brain samples. Total RNA was extracted using RNeasy Kit (QIAGEN), and 200 ng of RNA was used for reverse transcription using Superscript III (Invitrogen) according to the manufacturer's instructions. For analysis of transcript levels, real-time PCR was performed using SYBR Green Fast PCR master mix (Applied Biosystems). For analysis of splicing, PCR was performed using Immomix (Bioline) using the primers listed in Supplemental Table S2. The PCR products were visualized using QIAxcel capillary electrophoresis system (QIAGEN). To calculate exon inclusion ( $\Psi$ ), the percentage of the peak representing exon inclusion was divided by the total percentage of peaks representing exon inclusion and skipping. Splicing change was calculated by subtracting the exon inclusion in the knockdown cells from the inclusion in wild-type cells (thus, a positive  $\Delta\Psi$  represents exons enhanced by TARDBP, and negative those silenced by TARDBP).

### Gene Ontology (GO) analysis

GO term enrichment analysis was performed on exons with  $\text{DAR} < 1.2$  (2018 exons) to represent age-related splicing events, and on exons with  $\text{DAR} > 2$  (1532 exons) to represent disease-specific splicing events. These cut-offs were chosen in order to sample similarly sized data sets from opposite extremes of the age-related and disease-specific splicing spectrum. To make GO annotation exon-centric, we multiplied each gene annotation record to in-



clude all exons on the splicing microarray for the gene. For example, if gene X is annotated to GO term T and there are probes for five exons in gene X, the expanded annotation would include five records (gene X, exon 1), . . . , (gene X, exon 5) that would all be assigned to term T. Binomial distribution was then used to compute the probability  $[\Pr(K \geq k)]$  of observing  $k$  or more exons annotated to GO term among all  $n$  exons identified as differentially expressed in the experiment. If  $m$  is the number of all exons assigned to a GO term and  $N$  is the total number of exons measured in the experiment (control set), then

$$\Pr(K \geq k) = \sum_{i=k}^n \binom{n}{i} p^i (1-p)^{n-i},$$

$$\text{for } p = \frac{m}{N}.$$

### Statistical analyses

Hierarchical clustering of microarray data was performed using the HCLUST function in R based on the Euclidean distance between samples (calculated using the DIST function in R). Hierarchical clustering was performed on the 1000 exons with the most significant  $P$ -values in a two-tailed, Student's  $t$ -test between three FTLD-TDP individuals (ages 57–64 yr) and age-matched, cognitively normal individuals (ages 49–65 yr). Similar results were observed whether a more restricted set of exons (the 100 most significant) or all exons were used (data not shown). Statistical correction for the effects of technical covariables (sex and post-mortem delay) did not markedly affect these results. The 1000 exons with most significant splicing change in comparison of FTLD-TDP versus cognitively normal samples had highly significant overlap between the uncorrected and corrected sets (binomial distribution,  $P < 1 \times 10^{-43}$ ). Therefore, all analyses on the microarray data were performed on the uncorrected data set, because the limited number of samples and the uneven distribution of technical covariates between the different sample types made the correction of technical covariates prone to introducing analytical artifacts.

Principal component analysis (PCA) was performed on 13 exons assayed by RT-PCR across all samples using the PRCOMP function in R. We corrected for technical covariates (sex and post-mortem delay) in the PCA of RT-PCR values because the large number of samples and distribution of the covariates among those samples reduced the possibility of introducing analytical artifacts. We corrected for the effects of sex and post-mortem delay using the linear regression function LM in R as follows:

$$I_{jk} = \mu_j + S_{jk} + P_{jk} + \varepsilon_{jk},$$

where  $I_{jk}$  is the RT-PCR measured inclusion of exon  $j$  from sample  $k$ ,  $\mu_j$  is the mean inclusion of exon  $j$  across all samples,  $S_{jk}$  is a variable representing the effect of the sex of sample  $k$  on exon  $j$  inclusion,  $P_{jk}$  is a continuous variable representing the effect of post-mortem delay of sample  $k$  on exon  $j$  inclusion, and  $\varepsilon_{jk}$  is the residual for exon  $j$  from sample  $k$ . PCA was performed on the matrix of residuals  $\varepsilon$ . Bootstrap analysis and random sampling without replacement suggested that the PCA results are not the result of individual, outlier exons (median  $r$ ) (Supplemental Fig. 1E).

For analysis of age-related or disease-related changes, a  $P$ -value  $< 0.001$  was required (two-tailed Student's  $t$ -test, unequal variance), and a minimal twofold transcript-level change or a 20% change in proportion of exon including isoform. In Table 1, two additional genes are shown that do not satisfy this requirement: the *PTBP1* gene was included even though the change

was 1.8-fold, and *NOVA1* was included even though the  $P$ -value was 0.002.

### Data access

The microarray data from this study have been submitted to ArrayExpress (<http://www.ebi.ac.uk/arrayexpress/>) under accession no. E-MTAB-656. We also designed a web server for visualization and analysis of the microarray data, which can be accessed at <http://www.birolab.si/aspirebrain>.

### Acknowledgments

We thank Julian König for his valuable comments on the manuscript. This work was supported by the European Research Council grant (206726-CLIP), the Medical Research Council (MRC), the Slovenian Research Agency (P2-0209, J2-2197, L2-1112, Z7-3665), and a Wellcome Trust and Medical Research Council Strategic Grant Award (089701/Z/09/Z).

*Authors' contributions:* J.R.T. performed the microarray and RT-PCR validations; Z.W. did NOVA expression and RT-PCR validation of NOVA-target exons; and Z.W. and B.R. performed the immunoblot experiments. T.H. did the clinicopathological analysis and prepared the tissue samples; J.T.W. and K.Z. did statistical analyses; M.K., T.C., and G.R. analyzed the microarray data; T.A.C. and A.C.S. designed and provided the microarrays; B.Z., C.E.S., and J.U. supervised the studies; and J.R.T., B.R., C.E.S., K.Z., and J.U. wrote the paper in consultation with all other authors.

### References

- Almeida A, Moncada S, Bolanos JP. 2004. Nitric oxide switches on glycolysis through the AMP protein kinase and 6-phosphofructo-2-kinase pathway. *Nat Cell Biol* **6**: 45–51.
- Anderson P, Kedersha N. 2002. Visibly stressed: the role of eIF2, TIA-1, and stress granules in protein translation. *Cell Stress Chaperones* **7**: 213–221.
- Anthony K, Gallo JM. 2010. Aberrant RNA processing events in neurological disorders. *Brain Res* **1338**: 67–77.
- Baker M, Mackenzie IR, Pickering-Brown SM, Gass J, Rademakers R, Lindholm C, Snowden J, Adamson J, Sadovnick AD, Rollinson S, et al. 2006. Mutations in progranulin cause tau-negative frontotemporal dementia linked to chromosome 17. *Nature* **442**: 916–919.
- Bishop NA, Lu T, Yankner BA. 2010. Neural mechanisms of ageing and cognitive decline. *Nature* **464**: 529–535.
- Boutz PL, Chawla G, Stoilov P, Black DL. 2007a. MicroRNAs regulate the expression of the alternative splicing factor nPTB during muscle development. *Genes Dev* **21**: 71–84.
- Boutz PL, Stoilov P, Li Q, Lin CH, Chawla G, Ostrow K, Shiue L, Ares M Jr, Black DL. 2007b. A post-transcriptional regulatory switch in polypyrimidine tract-binding proteins reprograms alternative splicing in developing neurons. *Genes Dev* **21**: 1636–1652.
- Brooks WM, Lynch PJ, Ingle CC, Hatton A, Emson PC, Faull RL, Starkey MP. 2007. Gene expression profiles of metabolic enzyme transcripts in Alzheimer's disease. *Brain Res* **1127**: 127–135.
- Buckanovich RJ, Yang YY, Darnell RB. 1996. The onconeural antigen Nova-1 is a neuron-specific RNA-binding protein, the activity of which is inhibited by paraneoplastic antibodies. *J Neurosci* **16**: 1114–1122.
- Cahoy JD, Emery B, Kaushal A, Foo LC, Zamanian JL, Christopherson KS, Xing Y, Lubischer JL, Krieg PA, Krupenko SA, et al. 2008. A transcriptome database for astrocytes, neurons, and oligodendrocytes: A new resource for understanding brain development and function. *J Neurosci* **28**: 264–278.
- Cruts M, Gijssels I, van der Zee J, Engelborghs S, Wils H, Pirici D, Rademakers R, Vandenberghe R, Dermaut B, Martin JJ, et al. 2006. Null mutations in progranulin cause ubiquitin-positive frontotemporal dementia linked to chromosome 17q21. *Nature* **442**: 920–924.
- de Brito OM, Scorrano L. 2008. Mitofusin 2 tethers endoplasmic reticulum to mitochondria. *Nature* **456**: 605–610.
- Erraji-Benchekroun L, Underwood MD, Arango V, Galfalvy H, Pavlidis P, Smyrniotopoulos P, Mann JJ, Sibille E. 2005. Molecular aging in human

- prefrontal cortex is selective and continuous throughout adult life. *Biol Psychiatry* **57**: 549–558.
- Glatz DC, Rujescu D, Tang Y, Berendt FJ, Hartmann AM, Faltraco F, Rosenberg C, Hulette C, Jellinger K, Hampel H, et al. 2006. The alternative splicing of tau exon 10 and its regulatory proteins CLK2 and TRA2-BETA1 changes in sporadic Alzheimer's disease. *J Neurochem* **96**: 635–644.
- Harold D, Abraham R, Hollingworth P, Sims R, Gerrish A, Hamshere ML, Pahwa JS, Moskva V, Dowzell K, Williams A, et al. 2009. Genome-wide association study identifies variants at CLU and PICALM associated with Alzheimer's disease. *Nat Genet* **41**: 1088–1093.
- Heinzen EL, Yoon W, Weale ME, Sen A, Wood NW, Burke JR, Welsh-Bohmer KA, Hulette CM, Sisodiya SM, Goldstein DB. 2007. Alternative ion channel splicing in mesial temporal lobe epilepsy and Alzheimer's disease. *Genome Biol* **8**: R32. doi: 10.1186/gb-2007-8-3-r32.
- Hutton M, Lendon CL, Rizzu P, Baker M, Froelich S, Houlden H, Pickering-Brown S, Chakraverty S, Isaacs A, Grover A, et al. 1998. Association of missense and 5'-splice-site mutations in tau with the inherited dementia FTDP-17. *Nature* **393**: 702–705.
- Jelen N, Ule J, Zivin M, Darnell RB. 2007. Evolution of Nova-dependent splicing regulation in the brain. *PLoS Genet* **3**: 1838–1847.
- Jensen KB, Dredge BK, Stefani G, Zhong R, Buckanovich RJ, Okano HJ, Yang YY, Darnell RB. 2000. Nova-1 regulates neuron-specific alternative splicing and is essential for neuronal viability. *Neuron* **25**: 359–371.
- König J, Zarnack K, Rot G, Curk T, Kayicki M, Zupan B, Turner DJ, Luscombe NM, Ule J. 2010. iCLIP reveals the function of hnRNP particles in splicing at individual nucleotide resolution. *Nat Struct Mol Biol* **17**: 909–915.
- Kwiatkowski TJ Jr, Bosco DA, Leclerc AL, Tamrazian E, Vanderburg CR, Russ C, Davis A, Gilchrist J, Kasarskis EJ, Munsat T, et al. 2009. Mutations in the FUS/ALS gene on chromosome 16 cause familial amyotrophic lateral sclerosis. *Science* **323**: 1205–1208.
- Lagier-Tourenne C, Polymenidou M, Cleveland DW. 2010. TARDBP and FUS/ALS: emerging roles in RNA processing and neurodegeneration. *Hum Mol Genet* **19**: R46–R64.
- Lee CK, Weindrich R, Prolla TA. 2000. Gene-expression profile of the ageing brain in mice. *Nat Genet* **25**: 294–297.
- Lee JW, Beebe K, Nangle LA, Jang J, Longo-Guess CM, Cook SA, Davison MT, Sundberg JP, Schimmel P, Ackerman SL. 2006. Editing-defective tRNA synthetase causes protein misfolding and neurodegeneration. *Nature* **443**: 50–55.
- Liang WS, Reiman EM, Valla J, Duncley T, Beach TG, Grover A, Niedzielko TL, Schneider LE, Mastroeni D, Caselli R, et al. 2008. Alzheimer's disease is associated with reduced expression of energy metabolism genes in posterior cingulate neurons. *Proc Natl Acad Sci* **105**: 4441–4446.
- Llorian M, Schwartz S, Clark TA, Hollander D, Tan LY, Spellman R, Gordon A, Schweitzer AC, de la Grange P, Ast G, et al. 2010. Position-dependent alternative splicing activity revealed by global profiling of alternative splicing events regulated by PTB. *Nat Struct Mol Biol* **17**: 1114–1123.
- Loerch PM, Lu T, Dakin KA, Vann JM, Isaacs A, Geula C, Wang J, Pan Y, Gabuzda DH, Li C, et al. 2008. Evolution of the aging brain transcriptome and synaptic regulation. *PLoS ONE* **3**: e3329. doi: 10.1371/journal.pone.0003329.
- Lu T, Pan Y, Kao SY, Li C, Kohane I, Chan J, Yankner BA. 2004. Gene regulation and DNA damage in the ageing human brain. *Nature* **429**: 883–891.
- Makeyev EV, Zhang J, Carrasco MA, Maniatis T. 2007. The MicroRNA miR-124 promotes neuronal differentiation by triggering brain-specific alternative pre-mRNA splicing. *Mol Cell* **27**: 435–448.
- Merkwirth C, Langer T. 2008. Mitofusin 2 builds a bridge between ER and mitochondria. *Cell* **135**: 1165–1167.
- Miller JA, Oldham MC, Geschwind DH. 2008. A systems level analysis of transcriptional changes in Alzheimer's disease and normal aging. *J Neurosci* **28**: 1410–1420.
- Miller JA, Horvath S, Geschwind DH. 2010. Divergence of human and mouse brain transcriptome highlights Alzheimer disease pathways. *Proc Natl Acad Sci* **107**: 12698–12703.
- Mitew S, Kirkcaldie MT, Halliday GM, Shepherd CE, Vickers JC, Dickson TC. 2010. Focal demyelination in Alzheimer's disease and transgenic mouse models. *Acta Neuropathol* **119**: 567–577.
- Munoz MJ, Perez Santangelo MS, Paronetto MP, de la Mata M, Pelisch F, Boireau S, Glover-Cutter K, Ben-Dov C, Blaustein M, Lozano JJ, et al. 2009. DNA damage regulates alternative splicing through inhibition of RNA polymerase II elongation. *Cell* **137**: 708–720.
- Nangaku M, Sato-Yoshitake R, Okada Y, Noda Y, Takemura R, Yamazaki H, Hirokawa N. 1994. KIF1B, a novel microtubule plus end-directed monomeric motor protein for transport of mitochondria. *Cell* **79**: 1209–1220.
- Neumann M, Sampathu DM, Kwong LK, Truax AC, Micsenyi MC, Chou TT, Bruce J, Schuck T, Grossman M, Clark CM, et al. 2006. Ubiquitinated TARDBP in frontotemporal lobar degeneration and amyotrophic lateral sclerosis. *Science* **314**: 130–133.
- Nishiyama A, Komitova M, Suzuki R, Zhu X. 2009. Polydendrocytes (NG2 cells): multifunctional cells with lineage plasticity. *Nat Rev Neurosci* **10**: 9–22.
- Oprea GE, Krober S, McWhorter ML, Rossoll W, Muller S, Krawczak M, Bassell GJ, Beattie CE, Wirth B. 2008. Plastin 3 is a protective modifier of autosomal recessive spinal muscular atrophy. *Science* **320**: 524–527.
- Pegoraro G, Kubben N, Wickert U, Gohler H, Hoffmann K, Misteli T. 2009. Ageing-related chromatin defects through loss of the NURD complex. *Nat Cell Biol* **11**: 1261–1267.
- Poorkaj P, Bird TD, Wijsman E, Nemens E, Garruto RM, Anderson L, Andreadis A, Wiederholt WC, Raskind M, Schellenberg GD. 1998. Tau is a candidate gene for chromosome 17 frontotemporal dementia. *Ann Neurol* **43**: 815–825.
- Racca C, Gardiol A, Eom T, Ule J, Triller A, Darnell RB. 2010. The neuronal splicing factor nova co-localizes with target RNAs in the dendrite. *Front Neural Circuits* **4**: 5. doi: 10.3389/neuro.04.005.2010.
- Rideau AP, Gooding C, Simpson PJ, Monie TP, Lorenz M, Huttelmaier S, Singer RH, Matthews S, Curry S, Smith CW. 2006. A peptide motif in Raver1 mediates splicing repression by interaction with the PTB RRM2 domain. *Nat Struct Mol Biol* **13**: 839–848.
- Ruggiu M, Herbst R, Kim N, Jevsek M, Fak JJ, Mann MA, Fischbach G, Burden SJ, Darnell RB. 2009. Rescuing Z+ agrin splicing in Nova null mice restores synapse formation and unmasks a physiologic defect in motor neuron firing. *Proc Natl Acad Sci* **106**: 3513–3518.
- Scaffidi P, Misteli T. 2006. Lamin A-dependent nuclear defects in human aging. *Science* **312**: 1059–1063.
- Schlisio S, Kenchappa RS, Vredevelde LC, George RE, Stewart R, Greulich H, Shahriari K, Nguyen NV, Pigny P, Dahia PL, et al. 2008. The kinesin KIF1B acts downstream from EglN3 to induce apoptosis and is a potential p36 tumor suppressor. *Genes Dev* **22**: 884–893.
- Somel M, Guo S, Fu N, Yan Z, Hu HY, Xu Y, Yuan Y, Ning Z, Hu Y, Menzel C, et al. 2010. MicroRNA, mRNA, and protein expression link development and aging in human and macaque brain. *Genome Res* **20**: 1207–1218.
- Spellman R, Llorian M, Smith CW. 2007. Crossregulation and functional redundancy among the splicing regulator PTB and its paralogs nPTB and ROD1. *Mol Cell* **27**: 420–434.
- Spillantini MG, Murrell JR, Goedert M, Farlow MR, Klug A, Ghetti B. 1998. Mutation in the tau gene in familial multiple system tauopathy with presenile dementia. *Proc Natl Acad Sci* **95**: 7737–7741.
- Su B, Wang X, Nunomura A, Moreira PI, Lee HG, Perry G, Smith MA, Zhu X. 2008. Oxidative stress signaling in Alzheimer's disease. *Curr Alzheimer Res* **5**: 525–532.
- Tollervy JR, Curk T, Rogelj B, Briese M, Cereda M, Kayicki M, König J, Hortobagyi T, Nishimura AL, Zupunski V, et al. 2011. Characterizing the RNA targets and position-dependent splicing regulation by TARDBP. *Nat Neurosci* **14**: 452–458.
- Trioulier Y, Torch S, Blot B, Cristina N, Chatellard-Causse C, Verna JM, Sadoul R. 2004. Alix, a protein regulating endosomal trafficking, is involved in neuronal death. *J Biol Chem* **279**: 2046–2052.
- Twine NA, Janitz K, Wilkins MR, Janitz M. 2011. Whole transcriptome sequencing reveals gene expression and splicing differences in brain regions affected by Alzheimer's disease. *PLoS ONE* **6**: e16266. doi: 10.1371/journal.pone.0016266.
- Ule J, Jensen KB, Ruggiu M, Mele A, Ule A, Darnell RB. 2003. CLIP identifies Nova-regulated RNA networks in the brain. *Science* **302**: 1212–1215.
- Ule J, Ule A, Spencer J, Williams A, Hu JS, Cline M, Wang H, Clark T, Fraser C, Ruggiu M, et al. 2005. Nova regulates brain-specific splicing to shape the synapse. *Nat Genet* **37**: 844–852.
- Ule J, Stefani G, Mele A, Ruggiu M, Wang X, Taneri B, Gaasterland T, Blencowe BJ, Darnell RB. 2006. An RNA map predicting Nova-dependent splicing regulation. *Nature* **444**: 580–586.
- van der Zee J, Sleegers K, Van Broeckhoven C. 2008. Invited article: The Alzheimer disease-frontotemporal lobar degeneration spectrum. *Neurology* **71**: 1191–1197.
- Vance C, Rogelj B, Hortobágyi T, Shaw CE. 2009. Mutations in FUS, an RNA processing protein, cause familial amyotrophic lateral sclerosis type 6. *Science* **323**: 1208–1211.
- Wang Z, Kayicki M, Briese M, Zarnack K, Luscombe NM, Rot G, Zupan B, Curk T, Ule J. 2010. iCLIP predicts the dual splicing effects of TIA-RNA interactions. *PLoS Biol* **8**: e1000530. doi: 10.1371/journal.pbio.1000530.
- Whitwell JL, Jack CR Jr, Pankratz VS, Parisi JE, Knopman DS, Boeve BF, Petersen RC, Dickson DW, Josephs KA. 2008. Rates of brain atrophy over time in autopsy-proven frontotemporal dementia and Alzheimer disease. *Neuroimage* **39**: 1034–1040.

- Zahn JM, Poosala S, Owen AB, Ingram DK, Lustig A, Carter A, Weeraratna AT, Taub DD, Gorospe M, Mazan-Mamczarz K, et al. 2007. AGEMAP: A gene expression database for aging in mice. *PLoS Genet* **3**: e201. doi: 10.1371/journal.pgen.0030201.
- Zhang Y, Zhou L, Miller CA. 1998. A splicing variant of a death domain protein that is regulated by a mitogen-activated kinase is a substrate for c-Jun N-terminal kinase in the human central nervous system. *Proc Natl Acad Sci* **95**: 2586–2591.
- Zhang YJ, Xu YF, Dickey CA, Buratti E, Baralle F, Bailey R, Pickering-Brown S, Dickson D, Petrucelli L. 2007. Progranulin mediates caspase-dependent cleavage of TAR DNA binding protein-43. *J Neurosci* **27**: 10530–10534.
- Zhang C, Frias MA, Mele A, Ruggiu M, Eom T, Marney CB, Wang H, Licatalosi DD, Fak JJ, Darnell RB. 2010. Integrative modeling defines the Nova splicing-regulatory network and its combinatorial controls. *Science* **329**: 439–443.
- Zhao C, Takita J, Tanaka Y, Setou M, Nakagawa T, Takeda S, Yang HW, Terada S, Nakata T, Takei Y, et al. 2001. Charcot-Marie-Tooth disease type 2A caused by mutation in a microtubule motor KIF1B $\beta$ . *Cell* **105**: 587–597.
- Zuchner S, Mersiyanova IV, Muglia M, Bissar-Tadmouri N, Rochelle J, Dadali EL, Zappia M, Nelis E, Patitucci A, Senderek J, et al. 2004. Mutations in the mitochondrial GTPase mitofusin 2 cause Charcot-Marie-Tooth neuropathy type 2A. *Nat Genet* **36**: 449–451.

Received February 14, 2011; accepted in revised form July 5, 2011.